Behavior of the electron temperature in nonuniform complex plasmas

I. Denysenko*
Complex Systems, School of Physics, The University of Sydney, Sydney, New South Wales 2006, Australia and School of Physics and Technology V. N. Karazin Kharkiv National University, 61077 Kharkiv, Ukraine

K. Ostrikov
Complex Systems, School of Physics, The University of Sydney, Sydney, New South Wales 2006, Australia

M. Y. Yu
Theoretical Physics I, Ruhr University, D-44780 Bochum, Germany

N. A. Azarenkov
School of Physics and Technology, V. N. Karazin Kharkiv National University, 4 Svobody square, 61077 Kharkiv, Ukraine
(Received 17 April 2006; published 12 September 2006)

The response of complex ionized gas systems to the presence of nonuniform distribution of charged grains is investigated using a kinetic model. Contrary to an existing view that the electron temperature inevitably increases in the grain-occupied region because of enhanced ionization to compensate for the electrons lost to the grains, it is shown that this happens only when the ionizing electric field increases in the electron depleted region. The results for two typical plasma systems suggest that when the ionizing electric field depends on the spatially averaged electron density, the electron temperature in the grain containing region can actually decrease.

DOI: 10.1103/PhysRevE.74.036402 PACS number(s): 52.25.Vy, 52.27.Lw, 52.77.Dq, 52.80.Pi

I. INTRODUCTION

The study of response of ionized gas systems to externally introduced or self-assembled grains is important in plasma physics, geophysics, astrophysics, nanoscience, etc. [1–6]. Since the grains (for convenience, in the following we shall refer to them as dusts) are negatively charged, their presence causes local electron depletion. The complex mixed-phase gas discharge system tends to balance the loss and creation of electrons and ions in the system by enhancing ionization. It is often believed that this is possible only if the electron temperature is higher in the dusty regions with depleted electron density and if $T_e^{mf} > T_e^{gf}$, where T_e^{mf} and T_e^{gf} are the electron temperatures in the dusty and dust-free, or void, regions, respectively [2,3,7]. This conclusion has been supported by observations in the laboratory and space plasmas (see, e.g., Refs. [8–11] and the references therein). However, the question is if this response is generic to all mixed-phase gas discharges remains open. The difficulty lies in the complex relationship between the ionizing electric field and the local electron temperature.

Using kinetic modeling of two representative systems, we show that the electron temperature in the dusty region need not be enhanced relative to that in the void region. In fact, T_e increases only when the ionization-sustaining electric field is locally enhanced in the region with depleted electron density. More importantly, if the ionizing electric field is allowed to depend on spatially averaged electron density, the electron temperature in the dusty region can decrease, in contrast to common expectation. Our results should be useful to the understanding of mixed-phase systems involving externally driven ionized gases and micro- and submicron-sized grains, such as that used in industrial processing [12].

We consider two representative complex plasma systems with different dependence of the magnitude of the ionizing electric field on the locally depleted electron number density in the dusty region. The first case models a capacitively coupled rf plasma where the ionizing electric field depends on the *local* electron density. This case applies to most of the dusty plasma experiments [2,3]. The second case models an inductively coupled rf plasma, where the ionizing electric field depends on the *spatially averaged* electron density. This case is relevant to discharges sustained by evanescent electric fields, as in inductively coupled and wave-driven plasmas commonly used for materials processing [13,14].

II. FORMULATION

We consider a large-area low-pressure rf argon discharge containing dust grains. The length L of the discharge is smaller than its radius R, so that we can assume that all plasma parameters depend only on the coordinate z perpendicular to the planes bounding the plasma slab. The discharge is maintained by an electric field $E(z,t) = E_p(z)\exp(i\omega t)$, where $\omega = 2\pi f_E$ and $f_E = 13.56$ MHz, $E_p(z)$ is the amplitude of the rf field. The applied frequency ω is assumed to be higher than the ion plasma frequency, so that ions do not respond to the rf field.

Two different cases for the electric field profile shall be studied. First, we consider a local dependence, namely when the electric field $E_p(z)$ depends on the local electron density $n_e(z)$, similar to that often used for dust-free capacitively coupled rf plasmas [13,15]. Second, we consider a spatially

*Corresponding author. Email address: idenysenko@yahoo.com

 ©2006 The American Physical Society

averaged dependence, namely when $E_p(z)$ depends on the spatially averaged electron density, similar to that often used for dust-free inductively coupled rf plasmas [13,16].

In the first case the electric field in the bulk of the plasma slab is [see Eqs. (4.2.27) and (4.2.28) of Ref. [13]

$$|E_p(z)| = |J_T| \frac{\omega_{pe}^2(z)}{\nu_m(z)\sigma_{dc}(z)} \left[\frac{\omega^2 + \nu_m^2(z)}{(\omega_{pe}^2(z) - \omega^2)^2 + \omega^2 \nu_m^2(z)} \right]^{1/2}, \tag{1}$$

where $\sigma_{dc}(z)=e^2 n_e(z)/[m_e \nu_m(z)]$, J_T is the (constant) total current through the plasma slab, and e and m_e are the electron charge and mass, respectively. ν_m is the effective rate of momentum transfer including electron-neutral and electron-dust collisions, and ω_{pe} is the electron plasma frequency.

In the second case we consider an inductively coupled plasma generated by an rf current j_θ flowing through a planar induction coil. It is assumed that the induction coil is located on the top of the discharge chamber and separated by a thick dielectric from the plasma. The inductively coupled plasma is assumed to be azimuthally symmetric. The rf current j_θ induces the rf electromagnetic field with the azimuthal (E_θ) component of the electric field and the radial (H_r) and the axial (H_z) components of the magnetic field.

The equation for the electric field E_θ is [17,18]

$$\partial_r \frac{1}{r} \partial_r (r E_\theta) + \partial_z^2 E_\theta + \left(\frac{\omega}{c} \right)^2 E_\theta = \frac{\omega_{pe}^2(z)\omega[\omega + i\nu_m(z)]}{c^2[\omega^2 + \nu_m^2(z)]} E_\theta. \tag{2}$$

Assuming that [17,18] $E_\theta \sim J_1(3.83r/R)$ and $|\partial_z k| \ll |k|^2$, where J_1 is the Bessel function of first order and r is the radial coordinate, one can get from Eq. (2) [18]

$$E_\theta(z) \sim \frac{D}{\sqrt{k(z)}} \exp\left(- \int_0^z k(y) dy \right), \tag{3}$$

where $k^2(z)=[\omega_{pe}(z)/c]^2[b+i\nu_m(z)/\omega]/[1+\nu_m^2(z)/\omega^2]$, $b=1+a[1+\nu_m^2(z)/\omega^2]$,

$$a = \left(\frac{c}{\omega_{pe}(z)} \right)^2 \left[\left(\frac{3.83}{R} \right)^2 - \left(\frac{\omega}{c} \right)^2 \right],$$

and D is a constant. From Eq. (3) it follows that

$$|E_p(z)|^2 = |E_\theta(z)|^2 \sim \frac{D^2}{\sqrt{k_1^2(z) + k_2^2(z)}} \exp\left(- 2 \int_0^z k_1(y) dy \right), \tag{4}$$

where

$$k_1 = \frac{\omega_{pe}(z)}{c} \left\{ \frac{b[1 + (1 + \nu_m^2(z)/(\omega^2 b^2))^{1/2}]}{2[1 + \nu_m^2(z)/\omega^2]} \right\}^{1/2}$$

and

$$k_2 = \frac{\omega_{pe}^2(z)}{2k_1(z)c^2} \frac{\nu_m(z)/\omega}{[1 + \nu_m^2(z)/\omega^2]}.$$

When the length of the inductively coupled plasma is smaller than its radius, Eq. (4) describes the spatial distribution of the amplitude of the rf electric field in the main part of discharge. From (4) one can see that $E_p(z)$ is an integral function of $n_e(z)$, i.e., the field depends on the electron density nonlocally. Moreover, in most of planar inductive sources the electric field can be approximated by a function of the spatially averaged electron density [13,17]

$$|E_p| = E_{p0} \exp(-\langle k_1 \rangle z), \tag{5}$$

where E_{p0} is a constant and

$$\langle k_1 \rangle^{-1} = \frac{c}{\langle \omega_{pe} \rangle} \left\{ \frac{2(1 + \langle \nu_m \rangle^2/\omega^2)}{b[1 + (1 + \langle \nu_m \rangle^2/(\omega^2 b^2))^{1/2}]} \right\}^{1/2}$$

is the skin depth, $\langle \omega_{pe} \rangle$ and $\langle \nu_m \rangle$ are the spatially averaged plasma frequency and momentum frequency, respectively.

The plasma consists of electrons, singly charged positive ions Ar^+, and negatively charged colloidal dust grains of uniform size. The ions, argon atoms, and dust grains are at room temperature. We assume that $\tau_d \gg \tau_{eq}$, where τ_d and τ_{eq} are the characteristic times of dust motion and establishment of the equilibrium state, respectively. Therefore, the massive dust grains can be treated as immobile. The linear Debye-Hückel potential can be taken as the dust shielding potential if the dust radius a_d is smaller than 1 μm [2]. When the field is determined by (1), the discharge is assumed to be symmetrical with respect of $z=L/2$ (the discharge midplane). Since the field variations are much faster than that of energy relaxation, one can assume that the isotropic part of the electron distribution is time independent [19]. To determine the electron energy distribution function (EEDF) we make use of the spherical harmonics expansion in the Lorentz approximation by neglecting terms beyond the first order [20]. The expansion is valid if the electric field is not too high, such that the energy exchange by an electron within a mean free path λ is small compared to the mean electron energy. That is, elastic collisions dominate over inelastic ones, and the scale of the plasma inhomogeneity exceeds λ.

To obtain the EEDF, we start with the homogeneous Boltzmann equation [20], applicable when the plasma size and neutral pressure are sufficiently large. Thus, for an argon plasma we have $p_0 \Lambda > 100$ mTorr cm [21], where p_0 is the neutral pressure in mTorr and Λ (in cm) is the size of the discharge. It is convenient to express the isotropic part of the electron energy distribution function f_0 and the corresponding Boltzmann equation in terms of the kinetic energy scaling u [22]. Accordingly, f_0 can be written as $f_0(u) = n_e(\mathbf{r}) F_0(u)$, where $n_e(\mathbf{r})$ is the electron density and F_0 satisfies the condition $\int F_0(u) u^{1/2} du = 1$. The corresponding homogeneous Boltzmann equation is then [20]

$$-\frac{2e}{3m_e} \frac{d}{du} \left(\frac{u^{3/2}}{\nu_m(u)} E_{\text{eff}}^2(u) \frac{dF_0}{du} \right) = S_{ea}(F_0) + S_{ee}(F_0) + S_{ed}(F_0), \tag{6}$$

where $E_{\text{eff}}=|E_p| \nu_m(u)/[2(\nu_m^2(u)+\omega^2)]^{1/2}$. The expressions for collision integrals $S_{ea}(F_0)$, $S_{ed}(F_0)$, and $S_{ee}(F_0)$ describing the electron-atom, electron-dust, and electron-electron collisions can be found elsewhere [23,24]. The corresponding electron temperature is given by $T_{\text{eff}}=(2/3)\int_0^\infty F_0(u) u^{3/2} du$.

To obtain $n_e(\mathbf{r})$, or $n_e(z)$ in the one-dimensional problem here, it is necessary to consider the overall grain balance in the discharge. At sufficiently high pressures, when the mean free paths are small compared to all the relevant dimensions, the particle flows Γ_α, where $\alpha=i$ and e for the ions and electrons, in the z direction are

$$\Gamma_\alpha = -D_\alpha \partial_z n_\alpha \pm \mu_\alpha E_s n_\alpha, \tag{7}$$

where E_s is the ambipolar electric field sustaining the quasineutrality of the plasma, and the + and − operations are for the ion and electron equations, respectively, and D_α and μ_α are the diffusion and mobility coefficients, respectively. In the steady state we have $\Gamma_e=\Gamma_i$.

The particle balance equation is

$$\partial_z \Gamma_\alpha = n_e \langle \nu^i \rangle - n_d n_\alpha K_{\alpha d}, \tag{8}$$

where $\langle \nu^i \rangle$ is the averaged ionization rate, and $K_{\alpha d}$ is the rate coefficient for collection of particle α by dust grains. The model also assumes that the quasineutrality condition

$$n_e + n_d |Z_d| = n_i \tag{9}$$

be satisfied. Here n_d and Z_d are the dust charge and density, respectively. The dust charge Z_d is obtained by assuming that the electron current on the dust grain is equal to the ion current [2]. The ion current is calculated using the expression derived by Lampe *et al.* [25].

In calculating the ion current on a dust grain, usually the standard orbital motion limited (OML) theory is used [2,3]. In cylindrical geometry the theory is applicable if the condition [26] $\lambda_{in} > r_p(-eV_p/T_i)^{1/2}$ is satisfied, where λ_{in} is the ion-mean free path, r_p is the cylindrical probe radius, V_p is the probe potential, and T_i is the ion temperature. The condition is obtained assuming that far away from the probe the ion energy is a small quantity compared with $|eV_p|$. Lampe *et al.* [25] obtained an expression for the ion current to a dust grain assuming that $\lambda_{in} \geqslant R_0$, where R_0 is determined from the condition $|U(R_0)| \approx T_i$, and $U(r)$ denotes the potential energy of ion-grain interaction. In the parameter regime $0.1 \leqslant \beta_T \leqslant 10$, typical for laboratory dusty plasmas, we have [27],

$$I_i \approx \sqrt{8\pi} a_d^2 n_i \upsilon_{Ti} \xi \tau [1 + 0.1 \xi \tau (\lambda_s/\lambda_{in})],$$

where $\xi=|Z_d|e^2/a_d T_{\text{eff}}$, $\beta_T=|Z_d|e^2/T_i\lambda_s$, $\tau=T_{\text{eff}}/T_i$, $\upsilon_{Ti}=\sqrt{T_i/m_i}$, m_i and n_i are the ion mass and number density, respectively, and λ_s is the screening length. For submicron grains the screening length is about a Debye length [2]. For typical dusty plasmas, one has $\xi \sim 1$ and $\tau \sim 100$, and collisions can affect grain charging even when the ion mean free path is an order of magnitude larger than the screening length [27].

Equations (7) and (8) have to be supplemented by appropriate boundary conditions. We assume that in the capacitively coupled plasma the electron and ion drift velocities vanish at the plasma center. At the plasma boundary in the both capacitively coupled and inductively coupled plasmas the drift velocities are equal to the Bohm velocity [13], defined by [28] $\upsilon_{Bi} \approx \sqrt{2e/m_i}[\int F_0(u) u^{-1/2} du]^{-1/2}$. Equations (6)–(9) are solved numerically. The details of the numerical method are given in Ref. [23].

III. RESULTS

Calculations have been carried out for plasma parameters close to that in Samsonov and Goree's experiments [8,9,29] and in many inductively coupled plasma sources [30,31]. We shall use the local electric field determined by Eq. (1), as well as the averaged electric field determined by Eq. (4).

A. Local electric field

First we consider the case when the electric field depends locally on $n_e(z)$. The profiles of n_e, E_p, and T_{eff} for different dust densities and E_p determined by Eq. (1) are shown in Figs. 1 and 2. In the case corresponding to Fig. 1, the dust density profile is given by $n_d=n_{d0}=$ const. at 0.33 cm $<z<$ 0.67 cm, and n_d decreases linearly to zero at $z=0.3$ cm and $z=0.7$ cm, where n_{d0} is the maximal dust density. This profile models the void [32]. The dust grains can also be concentrated at the center of the discharge, such as in the case of dust balls [33–36]. To model this configuration we assume $n_d=n_{d0}$ is constant at $z<0.37$ cm and $n_d=0$ for $z>0.4$ cm. The profiles of n_e, E_p, and T_{eff} for the case are shown in Fig. 2.

One can see from Figs. 1(a) and 2(a) that with the increase of the dust density the electron density in the dusty plasma region decreases in comparison with that in the neighboring dust-free region. This is due to an increase of the electron loss to the dust grains. With an increase of n_{d0}, the rf electric field increases in whole plasma slab [Figs. 1(b) and 2(b)]. Thus, ionization is increased, compensating for the electron loss to the dust grains. Thus, increase of E_p is accompanied by an increase of T_{eff} in the whole plasma system [Figs. 1(c) and 2(c)]. Furthermore, because of the local decrease of n_e due to the condition $|E_p(z)| \sim 1/n_e(z)$, the electric field in the dusty region is larger than that in the neighboring dust-free region. As a result, the effective electron temperature in the dusty region is larger than in the dust-free region.

It is also of interest to compare the electron energy distribution function in the dusty and void regions. One can see from Fig. 3 that the number of high energy electrons in the tail of the EEDF in the dusty region is higher than that in the void region, which is inconsistent with the increase of the electron temperature in the dusty region.

B. Averaged electric field

We have also carried out the calculations using the averaged E_p determined by Eq. (4). The profiles of n_e, E_p, and T_{eff} are shown in Fig. 4. Here, we present the case where the grains are in the plasma center [33–35]. From Fig. 4(a) one can see that with an increase of n_d the electron density maximum shifts to $z=0$ because of the barrier established by the dust grains at the center and of the nonuniform electric field. As in the case of the local dependence of the electric field discussed earlier, an increase of n_d causes the electric field in

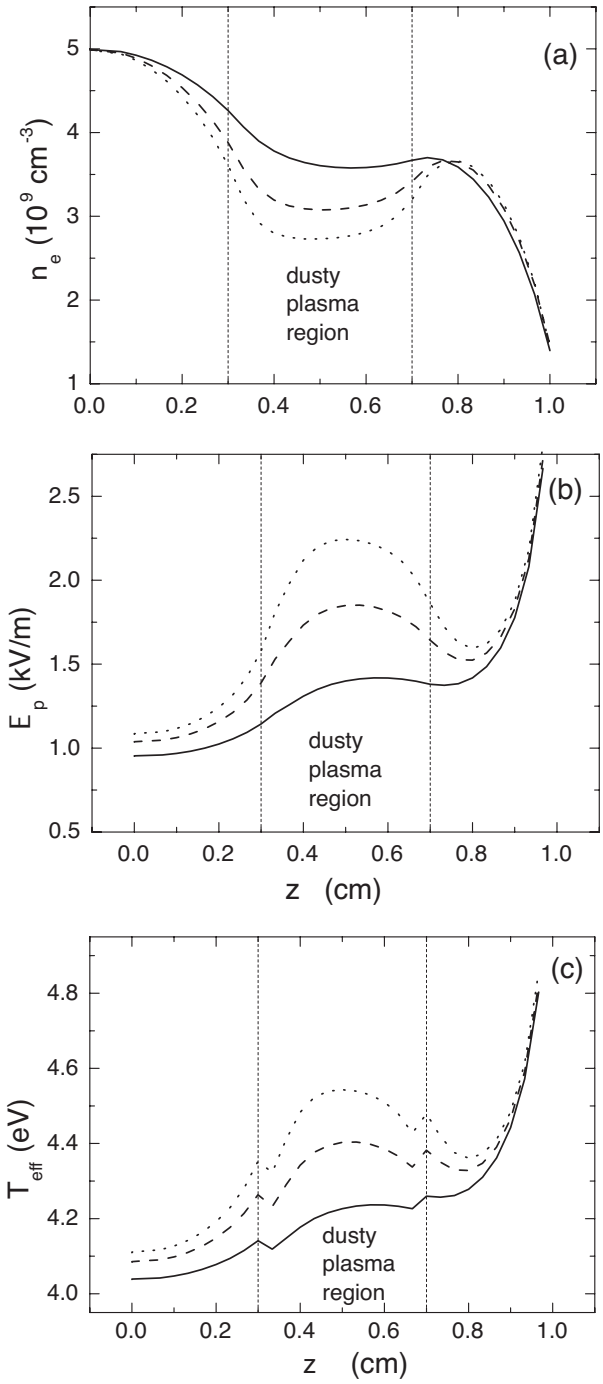

FIG. 1. The profiles of (a) n_e, (b) E_p, and (c) T_{eff} for the locally determined E_p of Eq. (1). The plasma parameters are $n_e(z=0)=5\times10^9$ cm^{-3}, $L/2=1$ cm, $a_d=175$ nm, $p_0=400$ mTorr, where $z=0$ is the slab midplane. The solid, dashed, and dotted curves are for $n_{d0}=10^7$, 2×10^7, and 3×10^7 cm^{-3}, respectively. A plasma with a center void is considered.

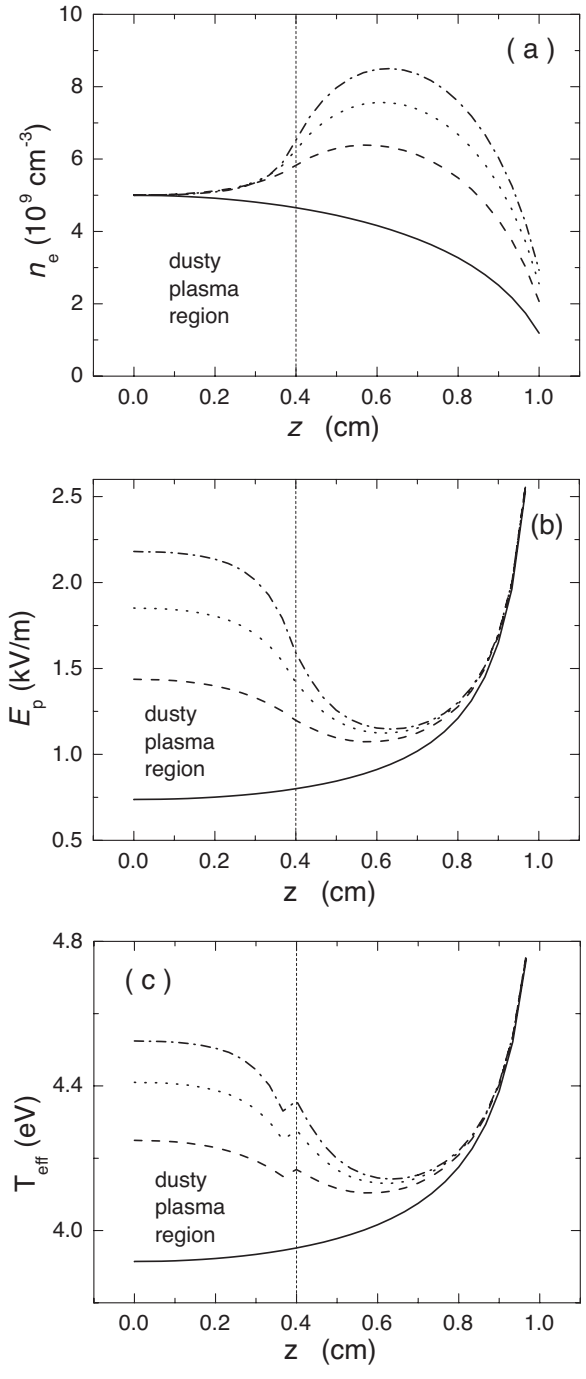

FIG. 2. The same as in Fig. 1 for the dust-ball case. The solid, dashed, dotted, and dash-dotted curves are for $n_{d0}=0.0, 10^7$, 2×10^7, and 3×10^7 cm^{-3}, respectively.

the whole system and the electron temperature in the dust-free regions to increase in order to compensate for the electron loss to the dusts, as shown in Figs. 4(b) and 4(c). However, in the present case of spatially averaged dependence, the electron temperature in the dusty region is smaller than that in the dust-free regions. The electron temperature does not increase in the dusty region because the electric field for the present case has an integral dependence on the electron density. As a result, the dust grains cannot significantly modify the local electric field profile, as shown in Fig. 4(b). The electric-field skin depth slightly increases with an increase of n_{d0} because of the decrease of the spatially averaged electron density. In the dusty region, T_{eff} decreases because of the collection of high-energy electrons by the grains

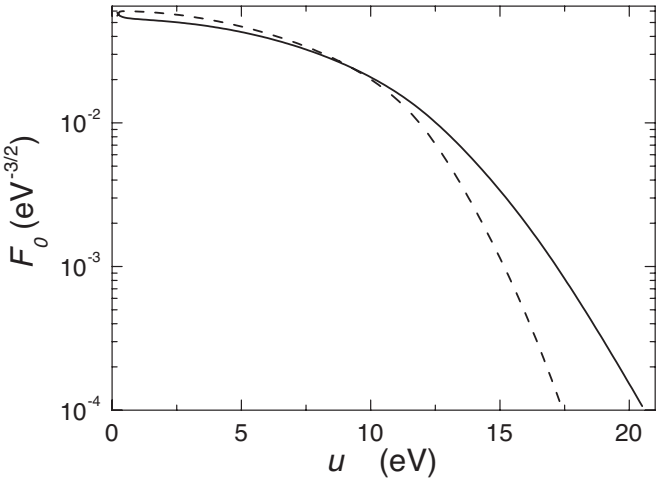

FIG. 3. The electron energy distribution functions at $z=0.1$ cm (dashed curve) and at $z=0.5$ cm (solid curve) for $n_{d0}=3\times10^7$ cm^{-3} and the dust density profile corresponding to the parameters of Fig. 1.

[23,37]. We note that even in the case of local dependence, T_{eff} can be smaller than the effective electron temperature in the neighboring dust-free regions. This can happen if $\omega_{pe}^2-\omega^2<\omega\nu_m$. It is of interest to point out that dust growth in a capacitively coupled $Ar/H_2/CH_4$ plasma accompanied by the electron temperature decrease has been reported recently [38].

IV. DISCUSSION AND SUMMARY

We now discuss the simplifications used in the modeling of the rf dusty plasma. First, we have assumed that the plasma is quasineutral. Thus the model may not be applicable for studying the formation of positive space-charge layers as well as double layers in dusty plasmas [39]. The double space-charge layer in the void has been studied by Annaratone *et al.* [40]. One can expect that double layers can also appear at dust-cloud boundaries near the chamber walls. In this case the double layers will probably affect the wall sheaths, and the Bohm criteria will have to be revised. The dust grains can also affect the sheath size as well as the power absorption in the sheaths [41,42]. However, the effects of voids and dust particles on the sheath behavior in a dusty plasma is beyond the scope of the present study. Moreover, the dust density profile is an external parameter here. That is, the spatial profile of the dust density has not been obtained self-consistently [35,36,39]. In fact, the dust distribution in a discharge depends on many factors, such as the chamber geometry, neutral gas pressure, grain size, input power, temperature of chamber walls [2,33], as well as the potentials of the surfaces surrounding the plasma [43,44]. On the other hand, the simplicity of our model allows one to understand the electron temperature nonuniformity in rf dusty plasmas.

In summary, complex ionized gas systems are strongly affected by the spatially nonuniform presence of dust grains by changing the spatial distribution of the effective electron temperature. The electron temperature profile is modified because of the dependence of the ionizing electric field on the electron density. If the electric field depends locally on the electron density, the presence of charged grains in the plasma changes the rf electric field and thus also the electron temperature distribution. For typical regimes of operation of capacitively coupled rf dusty plasmas, the electron temperature in the dusty region is larger than that in the neighboring void region since the rf electric field is inversely proportional to the local electron density. However, this behavior may not

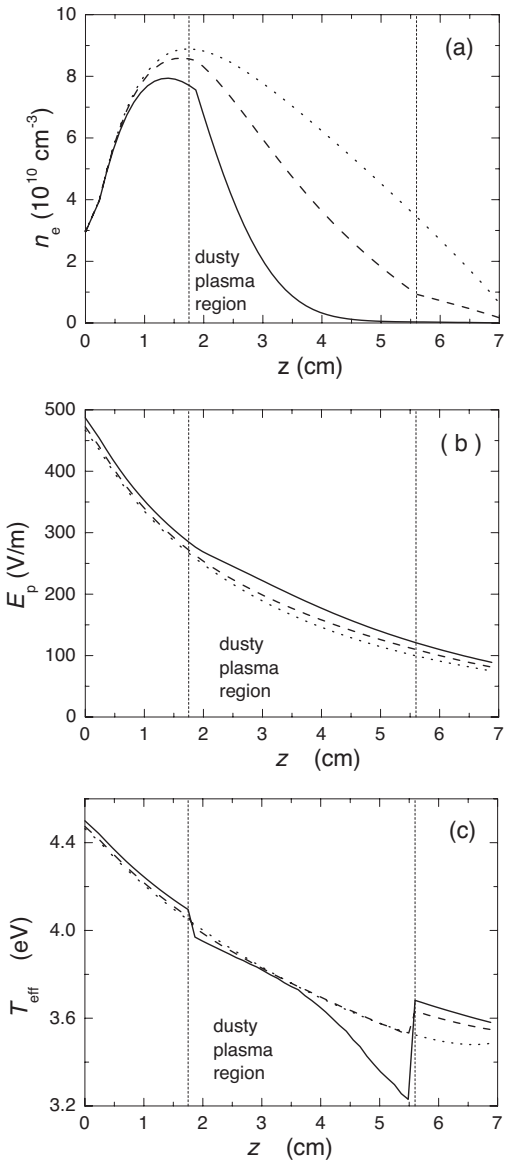

FIG. 4. The profiles of (a) n_e, (b) E_p, and (c) T_{eff} for the E_p profile determined by Eq. (4). The parameters are $n_e(z=0)=3\times10^{10}$ cm^{-3}, $L=7$ cm, $R=16$ cm, $a_d=100$ nm, $p_0=100$ mTorr, where $z=0$ is the plane where the inductive coils are located. The dust density profile is given by $n_d=n_{d0}=$const. at 1.87 cm$<z<$5.48 cm, and n_d decreases linearly to zero at $z=1.75$ cm and $z=5.6$ cm. The dotted, dashed, and solid curves are for $n_{d0}=0.0, 3\times10^6$, and 10^7 cm^{-3}, respectively.

occur for other systems. For example, in inductively coupled rf as well as wave-driven plasmas, the temperature in the dusty region may not be larger than that in the neighboring dust-free region where the rf electric field depends on the spatially averaged electron density and not on the local n_e. Thus the ionization characteristics are very important to the behavior of dusty discharges. The results here should be relevant to many applications, such as that in processing of submicron and micron grains [12] and for the understanding of many similar complex multiphase systems.

One of the authors (I.D.) was supported by the Humboldt Foundation. This work was partially supported by the Australian Research Council, and The University of Sydney.

[1] A. Gurevich and L. Pitaevsky, in *Reviews of Plasma Physics*, edited by M. Leontovich (Consultants Bureau, New York, 1980). Vol. 10.
[2] *Dusty Plasmas: Physics, Chemistry, and Technological Impacts in Plasma Processing*, edited by A. Bouchoule (Wiley, New York, 1999).
[3] S. V. Vladimirov and K. Ostrikov, Phys. Rep. **393**, 175 (2004).
[4] K. Ostrikov, Rev. Mod. Phys. **77**, 489 (2005).
[5] I. Stefanovic, E. Kovacevic, J. Berndt, and J. Winter, New J. Phys. **5**, 39.1 (2003).
[6] K. Ostrikov, I. B. Denysenko, S. V. Vladimirov, S. Xu, H. Sugai, and M. Y. Yu, Phys. Rev. E **67**, 056408 (2003).
[7] J. P. Boeuf, Phys. Rev. A **46**, 7910 (1992).
[8] D. Samsonov and J. Goree, Phys. Rev. E **59**, 1047 (1999).
[9] D. Samsonov and J. Goree, IEEE Trans. Plasma Sci. **27**, 76 (1999).
[10] C. Chen and W. A. Scales, J. Geophys. Res. **110**, A12313 (2005), and the references therein.
[11] S. I. Popel and A. A. Gisko, Nonlinear Processes Geophys. **13**, 223 (2006).
[12] E. Stoffels, W. W. Stoffels, H. Kersten, G. H. P. M. Swinkels, and G. M. W. Kroesen, Phys. Scr., T **T89**, 168 (2001); and the references therein.
[13] M. A. Lieberman and A. J. Lichtenberg, *Principles of Plasma Discharges and Materials Processing* (Wiley, New York, 1994).
[14] I. P. Ganachev and H. Sugai, Plasma Sources Sci. Technol. **11**, A178 (2002).
[15] O. A. Popov and V. A. Godyak, J. Appl. Phys. **59**, 1760 (1986).
[16] Yu. O. Tyshetskiy, A. I. Smolyakov, and V. A. Godyak, Phys. Rev. Lett. **90**, 255002 (2003).
[17] V. Vahedi, M. A. Lieberman, G. DiPeso, T. D. Rognlien, and D. Hewett, J. Appl. Phys. **78**, 1446 (1995).
[18] I. M. El-Fayoumi and I. R. Jones, Plasma Sources Sci. Technol. **7**, 162 (1998).
[19] U. Kortshagen, C. Busch, and L. D. Tsendin, Plasma Sources Sci. Technol. **5**, 1 (1996), and the references therein.
[20] I. P. Shkarofsky, T. W. Johnston, and M. P. Bachynski, *The Particle Kinetics of Plasmas* (Addison-Wesley, Reading, MA, 1966).
[21] U. Kortshagen, Plasma Sources Sci. Technol. **4**, 172 (1995).
[22] Yu. M. Aliev, H. Schlüter, and A. Shivarova, *Guided-Wave-Produced Plasmas* (Springer, Berlin, 2000).
[23] I. Denysenko, M. Y. Yu, K. Ostrikov, N. A. Azarenkov, and L. Stenflo, Phys. Plasmas **11**, 4959 (2004).
[24] I. Denysenko, M. Y. Yu, K. Ostrikov, and A. Smolyakov, Phys. Rev. E **70**, 046403 (2004).
[25] M. Lampe, R. Goswami, Z. Sternovsky, S. Robertson, V. Gavrishchaka, G. Ganguli, and G. Joyce, Phys. Plasmas **10**, 1500 (2003).
[26] B. M. Annaratone, M. W. Allen, and J. E. Allen, J. Phys. D **25**, 417 (1992).
[27] S. A. Khrapak, S. V. Ratynskaia, A. V. Zobnin, A. D. Usachev, V. V. Yaroshenko, M. H. Thoma, M. Kretschmer, H. Hofner, G. E. Morfill, O. F. Petrov, and V. E. Fortov, Phys. Rev. E **72**, 016406 (2005).
[28] J. T. Gudmundsson, Plasma Sources Sci. Technol. **10**, 76 (2001).
[29] J. Goree,(private communication). See also (dust voids in recent parabolic flight experiments): http://dusty.physics.uiowa.edu/%7Egoree/KC-135.html
[30] S. Xu, K. N. Ostrikov, Y. A. Li, E. L. Tsakadze, and I. R. Jones, Phys. Plasmas **8**, 2549 (2001).
[31] I. B. Denysenko, S. Xu, P. P. Rutkevych, J. D. Long, N. A. Azarenkov, and K. Ostrikov, J. Appl. Phys. **95**, 2713 (2004).
[32] M. Mikikian and L. Boufendi, Phys. Plasmas **11**, 3733 (2004).
[33] O. Arp, D. Block, A. Piel, and A. Melzer, Phys. Rev. Lett. **93**, 165004 (2004).
[34] Z. Chen, M. Y. Yu, and H. Luo, Phys. Scr. **71**, 638 (2005).
[35] Y. H. Liu, Z. Y. Chen, M. Y. Yu, L. Wang, and A. Bogaerts, Phys. Rev. E **73**, 047402 (2006).
[36] Y. Liu, S. Mao, Z.-X. Wang, and X. Wang, Phys. Plasmas **13**, 064502 (2006).
[37] M. J. McCaughey and M. J. Kushner, Appl. Phys. Lett. **55**, 951 (1989).
[38] F. J. Gordillo-Vazquez, M. Camero, and C. Gomez-Aleixandre, Plasma Sources Sci. Technol. **15**, 42 (2006).
[39] M. R. Akdim and W. J. Goedheer, Phys. Rev. E **67**, 066407 (2003); J. Appl. Phys. **94**, 104 (2003).
[40] B. M. Annaratone, S. A. Khrapak, P. Bryant, G. E. Morfill, H. Rothermel, H. M. Thomas, M. Zuzic, V. E. Fortov, V. I. Molotkov, A. P. Nefedov, S. Krikalev, and Yu. P. Semenov, Phys. Rev. E **66**, 056411 (2002).
[41] Ph. Belenguer, J. Ph. Blondeau, L. Boufendi, M. Toogood, A. Plain, A. Bouchoule, C. Laure, and J. P. Boeuf, Phys. Rev. A **46**, 7923 (1992).
[42] I. Denysenko, J. Berndt, E. Kovacevic, I. Stefanovic, V. Selenin, and J. Winter, Phys. Plasmas **13**, 073507 (2006).
[43] B. M. Annaratone, T. Antonova, D. D. Goldbeck, H. M. Thomas, and G. E. Morfill, Plasma Phys. Controlled Fusion **46**, B495 (2004).
[44] B. M. Annaratone, M. Glier, T. Stuffler, M. Raif, H. M. Thomas, and G. E. Morfill, New J. Phys. **5**, 92.1 (2003).